



**Sterically Demanding Methoxy and Methyl Groups in Ruthenium Complexes Lead to Enhanced Quantum Yields for Blue Light Triggered Photodissociation**

Journal:	<i>Dalton Transactions</i>
Manuscript ID	DT-ART-08-2018-003295.R1
Article Type:	Paper
Date Submitted by the Author:	27-Sep-2018
Complete List of Authors:	Qu, Fengrui; University of Alabama, Chem Martinez, Kristina; Tulane University, Department of Chemistry Arcidiacono, Ashley; Villanova University, Chemistry Park, Seungjo; The University of Alabama, Chemical and Biological Engineering Zeller, Matthias; Youngstown State University, Department of Chemistry Schmehl, Russel; Tulane University, Department of Chemistry Paul, Jared; Villanova University, Chemistry Kim, Yonghyun; The University of Alabama, Chemical and Biological Engineering Papish, Elizabeth; University of Alabama, Chem

**Sterically Demanding Methoxy and Methyl Groups in Ruthenium Complexes Lead to Enhanced Quantum Yields for Blue Light Triggered Photodissociation†**

*Fengrui Qu,<sup>a</sup> Kristina Martinez,<sup>b</sup> Ashley M. Arcidiacono,<sup>c</sup> Seungjo Park,<sup>d</sup> Matthias Zeller,<sup>e</sup> Russell H. Schmehl,<sup>b</sup> Jared J. Paul,<sup>\*c</sup> Yonghyun Kim,<sup>\*d</sup> Elizabeth T. Papish<sup>\*a</sup>*

<sup>a</sup>*Department of Chemistry, The University of Alabama, Tuscaloosa, AL 35487-0336, USA. E-mail: etpapish@ua.edu.*

<sup>b</sup>*Department of Chemistry, Tulane University, New Orleans, Louisiana 70118, United States*

<sup>c</sup>*Department of Chemistry, Villanova University, Villanova, PA 19085, USA. E-mail: jared.paul@villanova.edu.*

<sup>d</sup>*Department of Chemical and Biological Engineering, The University of Alabama, Tuscaloosa, AL 35487-0203, USA. E-mail: ykim@eng.ua.edu.*

<sup>e</sup>*Department of Chemistry, Purdue University, West Lafayette, IN 47907, USA*

†Electronic supplementary information (ESI) available: <sup>1</sup>H, <sup>13</sup>C NMR, IR, UV-vis spectra; methods and details of thermodynamic acidity (pK<sub>a</sub>) measurements; quantum yield measurement details; methodology for partition coefficient determination; structural parameters for X-ray crystallography. CCDC 1861548-1861549 contain the supplementary crystallographic data for this paper. These data can be obtained free of charge via [www.ccdc.cam.ac.uk/data\\_request/cif](http://www.ccdc.cam.ac.uk/data_request/cif), or by emailing [data\\_request@ccdc.cam.ac.uk](mailto:data_request@ccdc.cam.ac.uk), or by contacting The Cambridge Crystallographic Data Centre, 12 Union Road, Cambridge CB2 1EZ, UK; fax: +44 1223 336033.

**Abstract:**

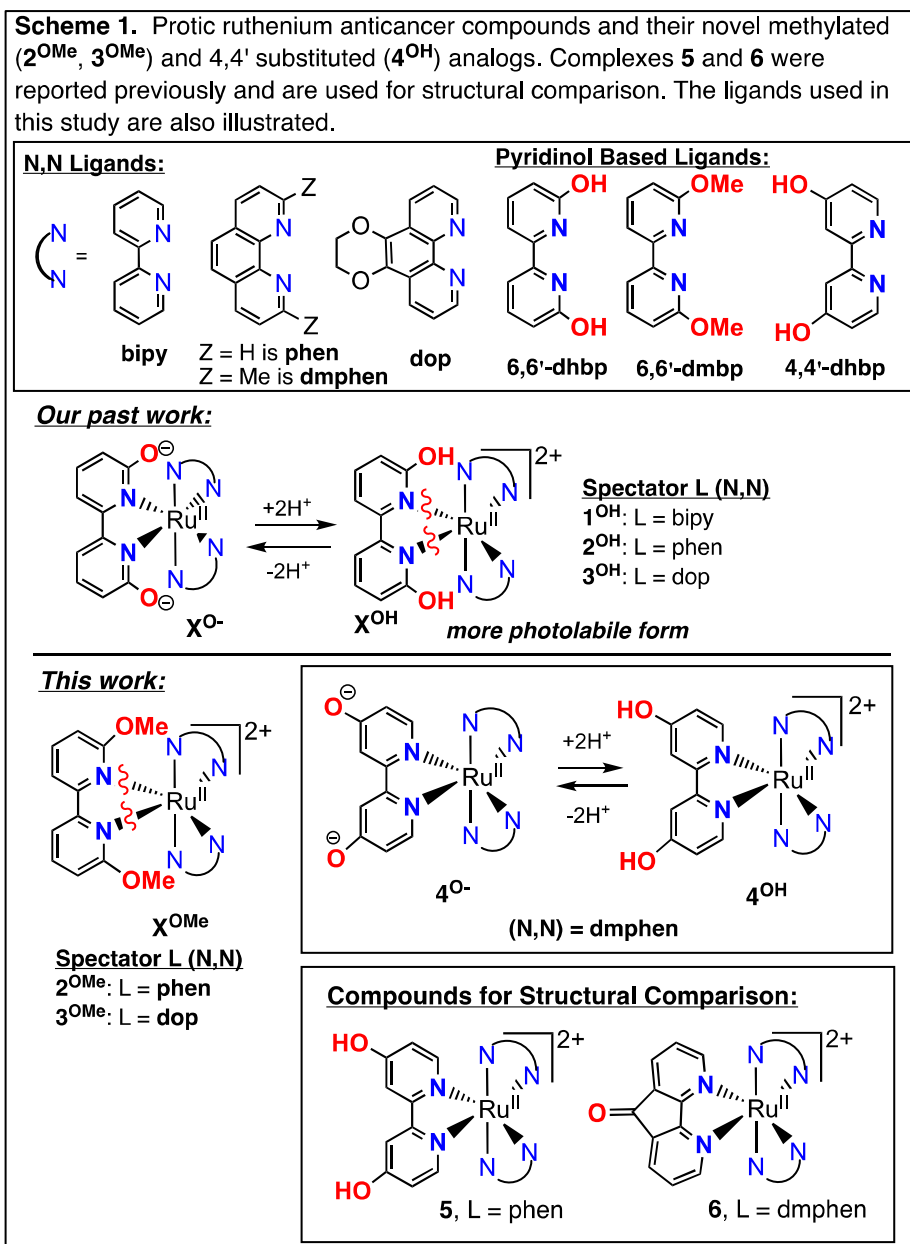
Ruthenium complexes containing a sterically congested metal center can serve as light activated prodrugs through photo-activated chemotherapy (PACT). In this work, we modified PACT agents containing 6,6'-dihydroxybipyridine (6,6'-dhbp) (Papish et al. *Inorg. Chem.* **2017**, *56*, 7519) by replacing it with a sterically bulky isoelectronic ligand, 6,6'-dimethoxybipyridine (6,6'-dmbp). The resulting complexes, [(phen)<sub>2</sub>Ru(6,6'-dmbp)]Cl<sub>2</sub> (**2**<sup>OMe</sup>, phen = 1,10-phenanthroline) and [(dop)<sub>2</sub>Ru(6,6'-dmbp)]Cl<sub>2</sub> (**3**<sup>OMe</sup>, dop = 2,3-dihydro-[1,4]dioxino[2,3-f][1,10]phenanthroline), have been fully characterized and display enhanced quantum yields for blue light triggered photodissociation of 0.024(6) and 0.0030(2), respectively. We have also synthesized **4**<sup>OH</sup> = [(dmphen)<sub>2</sub>Ru(4,4'-dhbp)]Cl<sub>2</sub> wherein dmphen = 2,9-dimethyl-1,10-phenanthroline and 4,4'-dhbp = 4,4'-dihydroxybipyridine. These ligands enhance steric bulk near the metal center and move the hydroxy groups further from the metal center, respectively. Complex **4**<sup>OH</sup> displays a relatively low quantum yield of 0.0014(2). All of the new complexes (**2**<sup>OMe</sup>, **3**<sup>OMe</sup>, **4**<sup>OH</sup>) were tested in breast cancer cells (MDA-MB-231) and were non-toxic (IC<sub>50</sub> >100 μM). This has been interpreted in terms of unfavorable log(D<sub>o/w</sub>) values and furthermore photodissociation alone is insufficient for cytotoxicity. We also report the crystal structures of **4**<sup>OH</sup> and **2**<sup>OMe</sup>, the thermodynamic acidity of complex **4**<sup>OH</sup>, and the redox potentials for all new complexes.

## Introduction

Ruthenium complexes with sterically bulky ligands are frequently used to trigger photodissociation for anticancer applications. Such ligand loss via photodissociation can lead to prodrug activation which can be used for photo-activated chemotherapy (PACT). (Abbreviations are listed here.<sup>1</sup>) Glazer *et al.* have made great progress in the use of Ru complexes that readily photodissociate a ligand to bind DNA and cause cytotoxicity.<sup>2-4</sup> These studies have used steric bulk near the metal center to destabilize the octahedral geometry and facilitate photolabilization of a ligand.<sup>3, 4</sup> The ligands dop, dmphen, and 2,2'-biquinoline are known to enhance photodissociation (with blue, red, or near-IR light) by causing strain in octahedral ruthenium complexes. Turro, Dunbar, and co-workers have used cytotoxic ligands (e.g. 5-cyanouracil with a ligand exchange quantum yield of 0.16) on Ru for light triggered release.<sup>5-8</sup> McFarland, Sadler, and others have shown that changing the charge of the metal complex (e.g. with cyclometallated C,N bound ligands) can greatly alter the cytotoxicity.<sup>9-13</sup> Collectively, these studies show that photodissociation to generate toxic byproducts (free metal, free ligand or both)<sup>14, 15</sup> plays a key role in the cytotoxicity of ruthenium prodrugs. However, another important factor is the uptake of these complexes as governed by charge and lipophilicity.<sup>16-18</sup>

Our initial effort in this area was the design of  $[(N,N)_2Ru(6,6'\text{-dhbp})]Cl_2$  complexes for PACT vs. cancerous cells wherein 6,6'-dhbp is a pH sensitive photolabile ligand (all ligands and metal complexes used in this work are shown in Scheme 1).<sup>19-21</sup> Upon irradiation with blue light ( $\lambda = 450$  nm),  $[(N,N)_2Ru(6,6'\text{-dhbp})]Cl_2$  forms the aqua complex,  $[(N,N)_2Ru(OH_2)_2]^{2+}$ , and 6,6'-dhbp. The spectator ligand, (N,N), was varied to include bipy ( $\mathbf{1}^{OH}$ ), phen ( $\mathbf{2}^{OH}$ ), and dop ( $\mathbf{3}^{OH}$ ) (Scheme 1). While complex  $\mathbf{3}^{OH}$  was the most cytotoxic ( $IC_{50} = \sim 4$   $\mu$ M vs. breast cancer cell lines) upon activation with blue light, this complex had a low quantum yield for photodissociation.<sup>19</sup> In fact, all three complexes ( $\mathbf{1}^{OH}$ - $\mathbf{3}^{OH}$ ) have low quantum yields on the order  $1 \times 10^{-3}$  when the complexes were at pH 5.0 (at this pH the complexes have OH groups and a 2+ charge) (Table 1 and Scheme 1). Admittedly, this pH value is below that found in the extracellular matrix in hypoxic tumors (pH 6.0-6.8),<sup>22</sup> and while this pH value is not biologically relevant it illustrates how the compound behaves as the more photolabile diprotic acid. These quantum yields are pH sensitive. For the most cytotoxic complexes  $\mathbf{2}^{OH}$  and  $\mathbf{3}^{OH}$ , the two  $pK_a$  values (reported in our prior work<sup>19</sup>) can be used to calculate the fraction which is fully protonated and more photolabile at pH 7.5. The Henderson-Hasselbach equation predicts that only 0.08 % of  $\mathbf{2}^{OH}$  and 0.05% of  $\mathbf{3}^{OH}$  bears OH groups (with a 2+ charge) at pH 7.5; the major species is neutral with O<sup>-</sup> groups ( $\mathbf{2}^{O^-}$  and  $\mathbf{3}^{O^-}$ , Scheme 1). Thus, under physiological conditions, the quantum yields are 1-2 orders of magnitude lower at pH 7.5 (vs. pH 5.0) (Table 1). Thus, we postulated that low quantum yields were limiting cytotoxicity and we aimed to synthesize complexes with increased quantum yields for photodissociation. Replacing OH groups with

OMe groups affords 100% of the complex in a photolabile form at physiological pH. In this work we describe the synthesis and properties of  $[(\text{phen})_2\text{Ru}(6,6'\text{-dmbp})]\text{Cl}_2$  ( $2^{\text{OMe}}$ ) and  $[(\text{dop})_2\text{Ru}(6,6'\text{-dmbp})]\text{Cl}_2$



( $3^{\text{OMe}}$ ) (Scheme 1).

**Table 1.** Comparison of acidity, quantum yields for photodissociation upon irradiation at 450 nm, and  $\log(D_{o/w})$  values, and  $E_{1/2}$  values for selected compounds discussed herein.

com- pound	structure	$pK_a$ avg	$\Phi_{PD}$ at pH 5.0 (mostly $X^{OH}$ if protic ligand)	$\Phi_{PD}$ at pH 7.5 (mostly $X^{O-}$ if protic ligand)	$\log(D_{o/w})$ at pH 7.4	$E_{1/2}$ (V)
<b>1<sup>OH</sup></b> , <sup>a</sup>	$[(bipy)_2Ru(6,6'-dhbp)]^{2+}$	6.3	0.0058(5)	0.0012(1)	1.4(1) <sup>a</sup>	1.12 <sup>b</sup>
<b>2<sup>OH</sup></b> , <sup>a</sup>	$[(phen)_2Ru(6,6'-dhbp)]^{2+}$	6.0(1)	0.0020(2)	0.000036(1)	1.6(1) <sup>a</sup>	--- <sup>c</sup>
<b>3<sup>OH</sup></b> , <sup>a</sup>	$[(dop)_2Ru(6,6'-dhbp)]^{2+}$	5.9(1)	0.001(1)	0.00022(3)	1.8(1) <sup>a</sup>	--- <sup>c</sup>
<b>2<sup>OMe</sup></b>	$[(phen)_2Ru(6,6'-dmbp)]Cl_2$	N/A	0.024(6)	---	-1.3(2)	0.99 <sup>d</sup>
<b>3<sup>OMe</sup></b>	$[(dop)_2Ru(6,6'-dmbp)]Cl_2$	N/A	0.0030(2)	---	-1.1(1)	0.98 <sup>d</sup>
<b>4<sup>OH</sup></b>	$[(dmphen)_2Ru(4,4'-dhbp)]Cl_2$	6.08(2)	0.0014(2)	---	0.58(2)	0.66 <sup>d</sup>

<sup>a</sup>All measurements on **1<sup>OH</sup>**, **2<sup>OH</sup>**, and **3<sup>OH</sup>** are from our prior work.<sup>19,20</sup> An improved procedure for measuring  $\log(D_{o/w})$  led to small changes in the observed values relative to our published prior work.<sup>19</sup>

<sup>b</sup>Versus SCE in acetonitrile.<sup>20</sup>

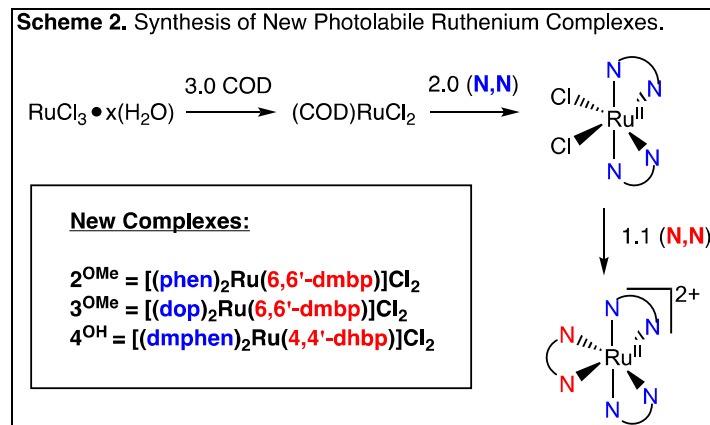
<sup>c</sup>Redox potentials for **2<sup>OH</sup>** and **3<sup>OH</sup>** were not measured.<sup>19</sup>

<sup>d</sup>Versus Ag/AgCl in aqueous solution at pH = 7.0 at a scan rate of 200mV/s.

Furthermore, we have also synthesized **4<sup>OH</sup>** =  $[(dmphen)_2Ru(4,4'-dhbp)]Cl_2$  to provide steric bulk from the dmphen ligand with four methyl groups near the metal center (Scheme 1). Six bulky groups cannot be accommodated near the metal center as such a complex (with 6,6'-dhbp) would be unstable; thus using the dmphen ligand necessitated moving the hydroxyl groups away from the metal center with 4,4'-dhbp. This complex **4<sup>OH</sup>** was designed to determine if such derivatives would have similar quantum yields or cytotoxicity to analogous complexes like **2<sup>OH</sup>**. All of the new complexes (**2<sup>OMe</sup>**, **3<sup>OMe</sup>**, **4<sup>OH</sup>**) were tested in breast cancer cells (MDA-MB-231) and were non-toxic ( $IC_{50} > 100 \mu M$ ) despite greatly improved quantum yields. This information has been interpreted in terms of unfavorable  $\log(D_{o/w})$  values reported herein that may lead to poor cellular uptake and furthermore photodissociation alone is insufficient for toxicity. Herein, octanol/water partition coefficients ( $\log(D_{o/w})$ ) are used to measure the hydrophilic (negative  $\log(D_{o/w})$ ) vs. lipophilic (positive  $\log(D_{o/w})$ ) character of our complexes and to estimate cellular uptake by passive diffusion. We also report the structures of **4<sup>OH</sup>** and **2<sup>OMe</sup>** as determined by Single Crystal X-Ray Diffraction and we report the thermodynamic acidity of complex **4<sup>OH</sup>**.

## Results and Discussion

**Synthesis and Characterization of the Metal Complexes.** The new metal complexes ( $2^{\text{OMe}}$ ,  $3^{\text{OMe}}$ ,  $4^{\text{OH}}$ ) were synthesized by modifying known procedures (Scheme 2).<sup>19, 20</sup> The N,N co-ligands (in blue, Scheme 2) were purchased (phen, dmphen) or synthesized (dop) using literature protocols.<sup>3</sup> These co-ligands are readily added to the 1,5-cyclooctadiene complex of ruthenium ((COD)RuCl<sub>2</sub>). The cis product, [(N,N)<sub>2</sub>RuCl<sub>2</sub>], was then treated with the oxygenated bipy ligand (6,6'-dmbp or 4,4'-dhbp, in red, Scheme 2). The final products were recrystallized by slow diffusion of diethyl ether into a solution of corresponding complexes in dry ethanol (for  $4^{\text{OH}}$ ) or acetonitrile (for  $2^{\text{OMe}}$  and  $3^{\text{OMe}}$ ) to afford the pure product. For  $4^{\text{OH}}$ , the complex was isolated as hexafluorophosphate salt, and then was converted to chloride salt by treating with excess of Et<sub>4</sub>NCl in acetone. All three products were fully characterized by <sup>1</sup>H- and <sup>13</sup>C-NMR, ESI-MS, IR, UV-Vis (see Figures S7-9 in the ESI), and elemental analysis. Single crystal X-Ray diffraction structures were obtained for compounds  $4^{\text{OH}}$  and  $2^{\text{OMe}}$ .



**X-Ray Crystallography.** Crystals suitable for single crystal XRD analysis of  $2^{\text{OMe}}$  were obtained by slow diffusion of diethyl ether into a MeCN solution of  $2^{\text{OMe}}$  (Figures 1, 2 and 3 and Table 2). The structure features a distorted octahedral geometry around the central metal, similar to its previously reported hydroxyl analogue  $2^{\text{OH}}$ , [(phen)<sub>2</sub>Ru(6,6'-dhbp)]Cl<sub>2</sub> (Figures 2 and 3).<sup>19</sup> The substitution of 6,6'-OH ( $2^{\text{OH}}$ ) with 6,6'-OMe on  $2^{\text{OMe}}$  did not disturb the geometric configuration around the central metal significantly. For example, the average Ru-N(6,6'-dmbp) distance in compound  $2^{\text{OMe}}$  (2.095(1)) is only slightly longer than the corresponding distances in the hydroxy analogue  $2^{\text{OH}}$  (Ru-N = 2.086(2)), suggesting a slight steric bulk increase for methoxy groups. All other bond distances, angles and torsion angles are similar between  $2^{\text{OH}}$  and  $2^{\text{OMe}}$ .

Crystals suitable for single crystal XRD analysis of  $4^{\text{OH}}$  were obtained by slow diffusion of diethyl ether into an ethanol solution of  $4^{\text{OH}}$  (Figures 1, 2 and 3 and Table 2). Compared to  $2^{\text{OH}}$ , the compound  $4^{\text{OH}}$ , [(dmphen)<sub>2</sub>Ru(4,4'-dhbp)]Cl<sub>2</sub>, shows some significant changes. Effectively, steric distortions are present in 6,6'-dhbp in  $2^{\text{OH}}$ , but these distortions are moved to the dmphen ligands in  $4^{\text{OH}}$ . The average

Ru-N (dmphen) bond distances = 2.101(1) Å are longer in  $\mathbf{4}^{\text{OH}}$  due to the methyl groups' steric bulk, cf. the Ru-N (phen) = 2.061(1) Å in  $\mathbf{2}^{\text{OH}}$ . In addition, the average Ru-N (4,4'-dhbp) bond distances = 2.092(3) in  $\mathbf{4}^{\text{OH}}$ , which are slightly longer than Ru-N (6,6'-dhbp) = 2.086(2) in  $\mathbf{2}^{\text{OH}}$ . Complex  $\mathbf{4}^{\text{OH}}$  does have OH $\cdots$ Cl $\cdots$  hydrogen bonds, but these do not alter the bond lengths appreciably (e.g. the C-O bond distances are ~1.34 Å in  $\mathbf{4}^{\text{OH}}$ , which are similar to analogous C-O distances in  $\mathbf{2}^{\text{OMe}}$ ,  $\mathbf{2}^{\text{OH}}$ , and other pyridinol derived Ru complexes<sup>23</sup>). In  $\mathbf{4}^{\text{OH}}$ , the steric bulk is less for the oxygenated bipy derivative, but the crowding from the methyl groups of the dmphen ligand serves to lengthen Ru-N (of 4,4'-dhbp) distances (cf.  $\mathbf{5} = [(\text{phen})_2\text{Ru}(4,4'\text{-dhbp})]^{2+}$  in Table 2). The torsion angle (5.6(4)°, Table 2) within the 4,4'-dhbp ring is much smaller than that for  $\mathbf{2}^{\text{OH}}$  (16.6(3)), due to the OH groups being in a less crowded position in 4,4'-dhbp. This can be clearly seen in the side-by-side comparison presented in Figure 2. The pyridinol rings are coplanar in  $\mathbf{4}^{\text{OH}}$  and 4,4'-dhbp lines up with the equatorial Ru-N plane, while the 6,6'-dhbp in  $\mathbf{2}^{\text{OH}}$  is tilted below the equatorial plane. Conversely, the torsion angle on the spectator ligand (17.8(2)°) in  $\mathbf{4}^{\text{OH}}$  is now larger than those in  $\mathbf{2}^{\text{OH}}$  (4.9(1)°), due to the steric hindrance from the methyl groups of dmphen. Thus,  $\mathbf{4}^{\text{OH}}$  is significantly more distorted from an octahedral geometry vs.  $\mathbf{2}^{\text{OH}}$ .

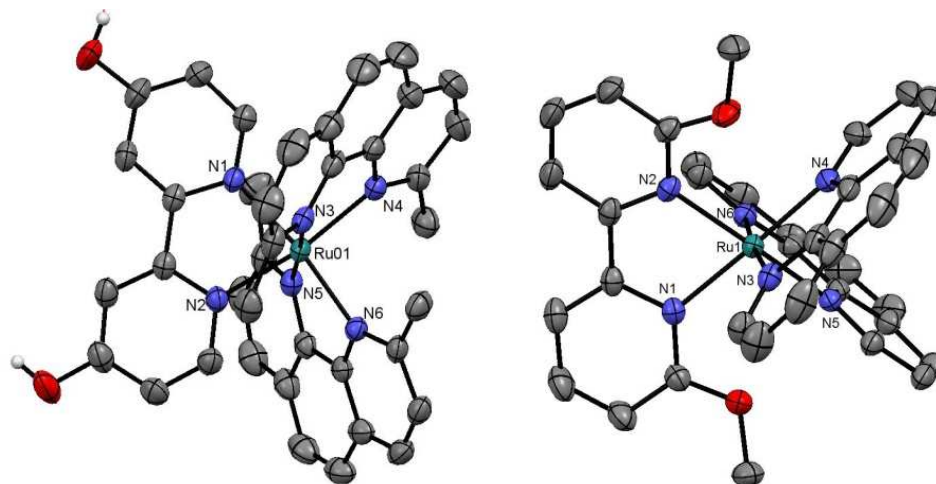


**Figure 1.** The ORTEP diagrams (with ellipsoids at 50% probability) of the cations of  $\mathbf{4}^{\text{OH}}$  (left) and  $\mathbf{2}^{\text{OMe}}$  (right). Hydrogen atoms (except that on oxygen) and chloride counter anions were omitted for clarity. Complex  $\mathbf{4}^{\text{OH}}$  contains no solvent molecules, but complex  $\mathbf{2}^{\text{OMe}}$  contains one water molecule per each Ru molecule, which is omitted for clarity. A full list of structural parameters is included in the Supporting Information.

We can also compare  $\mathbf{4}^{\text{OH}}$  to  $\mathbf{5}$ ,  $[(\text{phen})_2\text{Ru}(4,4'\text{-dhbp})]\text{Cl}_2$ , which was reported by us previously and only differs in removal of the methyl groups from the spectator ligands. Complex  $\mathbf{4}^{\text{OH}}$  is much more distorted than  $\mathbf{5}$  as shown in the torsion angles of the spectator ligands (Figure 2). This can also be seen in the trans angles (Table 2), which vary more for  $\mathbf{4}^{\text{OH}}$  as is evident from Figure 3. The highly-distorted structure of  $\mathbf{4}^{\text{OH}}$  favors photodissociation (*vide infra*), which is in direct contrast to  $\mathbf{5}$  (non-dissociative upon irradiation).

A crystal structure similar to **4<sup>OH</sup>** has been reported before (see Figure 2, compound **6**), namely, [(AFO)Ru(dmphen)<sub>2</sub>](ClO<sub>4</sub>)<sub>2</sub>, where AFO = 4,5-diazafluore-9-one.<sup>24</sup> Selected bond distances and angles of interest are summarized in Table 2 and presented in Figure 3 for comparison. The average Ru-N(dmphen) bond distance in **4<sup>OH</sup>** is essentially the same as the corresponding Ru-N(dmphen) bond distance in **6**, which are 2.101(1) and 2.097(3), respectively. As a contrast, the average Ru-N(dhbp) bond distance in **4<sup>OH</sup>** is significantly shorter than the corresponding Ru-N(AFO) bond distance in **6**, which are 2.092(3) and 2.143(5), respectively. The longer Ru-N(AFO) bond distances are probably due to electronic factors unique to the diazafluorenone ligand.

**Table 2.** Selected Bond Lengths and Angles of the Complexes **2<sup>OMe</sup>** and **4<sup>OH</sup>**, as compared to their structural analogues **2<sup>OH</sup>**, **5**, and **6**.

	<b>2<sup>OMe</sup></b>	<b>2<sup>OH</sup></b> <sup>a</sup>	<b>4<sup>OH</sup></b>	<b>5<sup>b</sup></b>	<b>6<sup>c</sup></b>
<b>Ru-N1</b>	2.087(1)	2.086(2)	2.089(2)	2.062(2)	2.148(4)
<b>Ru-N2</b>	2.103(1)	2.087(2)	2.094(2)	2.058(2)	2.138(3)
<b>Ru-N3</b>	2.060(1)	2.075(2)	2.095(2)	2.058(2)	2.109(5)
<b>Ru-N4</b>	2.054(1)	2.063(2)	2.105(2)	2.070(2)	2.080(3)
<b>Ru-N5</b>	2.064(1)	2.055(2)	2.113(2)	2.061(2)	2.102(4)
<b>Ru-N6</b>	2.074(1)	2.052(2)	2.089(2)	2.050(2)	2.098(5)
<b>Avg Ru-N</b>	2.074(1)	2.070(1)	2.098(1)	2.060(1)	2.113(2)
<b>Avg Ru-N (oxygenated N,N)</b>	2.095(1)	2.086(2)	2.092(3)	2.060(3)	2.143(5)
<b>Avg Ru-N ("spectator" N,N)</b>	2.063(1)	2.061(1)	2.101(1)	2.060(1)	2.097(3)
<b>N-Ru-N1</b>	174.86(5)	172.0(1)	170.71(8)	173.1(1)	171.0(2)
<b>N-Ru-N2</b>	171.15(4)	172.8(1)	171.73(8)	173.4(1)	173.9(2)
<b>N-Ru-N3</b>	175.42(5)	177.1(1)	176.10(8)	175.9(1)	176.9(2)
<b>Avg trans angle</b>	173.81(4)	174.0(1)	172.85(7)	174.1(1)	173.9(2)
<b>L1 torsion<sup>d</sup> (oxygenated N,N)</b>	16.4(1)	16.8(2)	-7.4(3)	-2.9(3)	-5.0(6)
	-14.5(1)	-16.4(2)	-3.8(3)	-5.2(3)	3.0(6)
<b>Avg  L1 torsion </b>	15.5(1)	16.6(3)	5.6(4)	4.1(4)	4.0(8)
<b>L2 torsion<sup>d</sup> ("spectator" N,N)</b>	-4.5(2)	4.1(2)	-21.5(3)	4.5(3)	-13.5(6)
	-0.5(2)	-4.5(2)	15.0(3)	-5.6(3)	11.0(6)
<b>L3 torsion<sup>d</sup> ("spectator" N,N)</b>	-2.9(1)	-6.0(2)	-20.6(3)	-5.2(3)	15.9(6)
	-2.3(1)	5.0(2)	13.9(3)	5.1(3)	-20.1(5)
<b>Avg  L2 or L3 torsion<sup>d</sup> </b>	2.6(1)	4.9(1)	17.8(2)	5.1(2)	15.1(4)

<sup>a</sup>Data for **2<sup>OH</sup>** = [(phen)<sub>2</sub>Ru(6,6'-dhbp)]Cl<sub>2</sub> has been previously reported.<sup>19</sup>

<sup>b</sup>Data for **5** = [(phen)<sub>2</sub>Ru(4,4'-dhbp)]Cl<sub>2</sub> has been previously reported.<sup>19</sup>

<sup>c</sup>Data for **6** = [Ru(dmphen)<sub>2</sub>(AFO)]<sup>2+</sup> was reproduced from the literature.<sup>24</sup>

<sup>d</sup>These torsion angles are for Ru-N-C-C' and Ru-N'-C'-C and they involve the C and C' atoms which connect the pyridine derived rings.

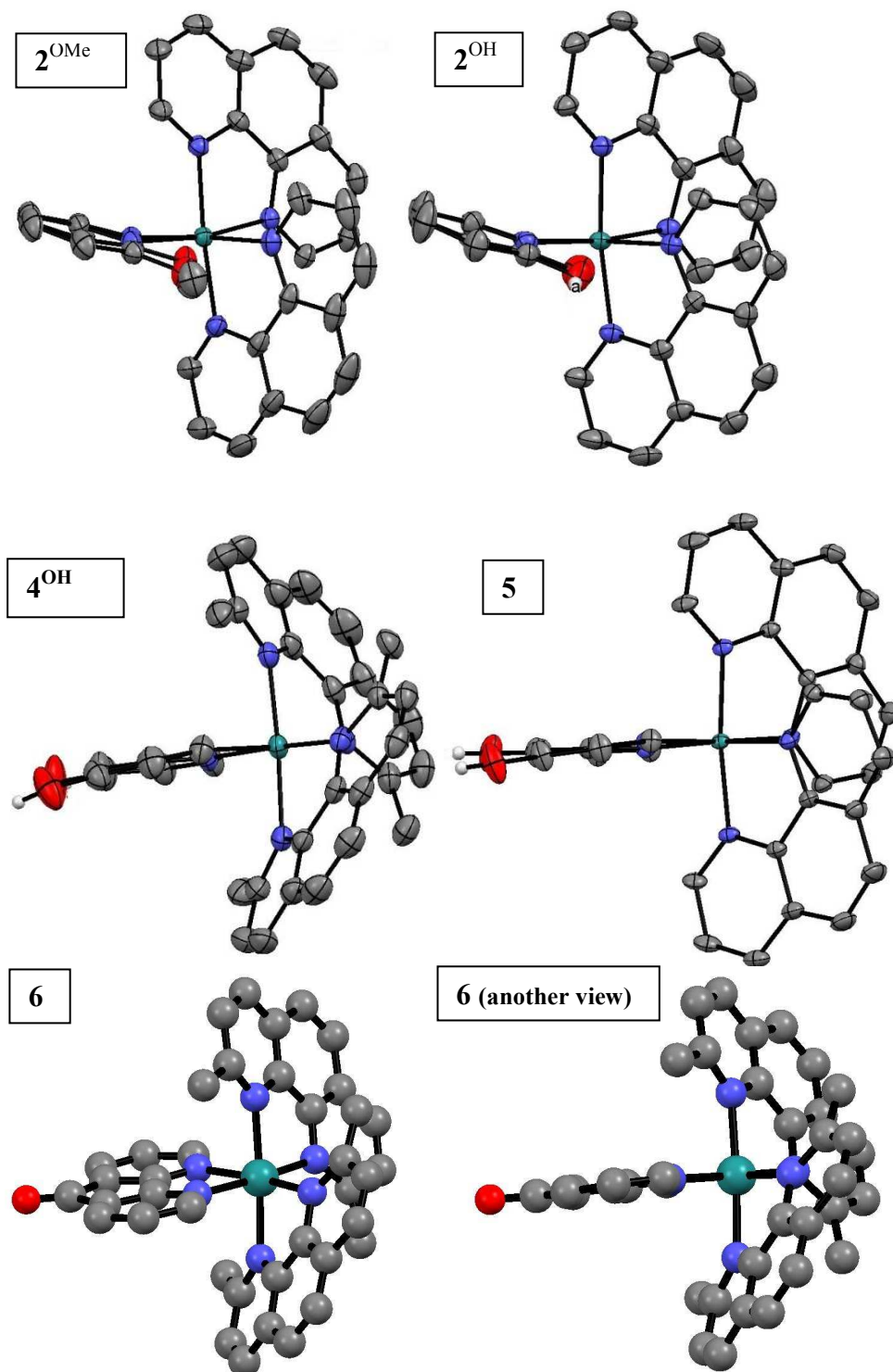


**Figure 2.** A comparison of crystal structures of the complexes 2<sup>OMe</sup>, 2<sup>OH</sup>, 4<sup>OH</sup>, 5 and 6. Structure 6 was reproduced from literature.<sup>24</sup> Note: Thermal ellipsoid data are not available for 6.

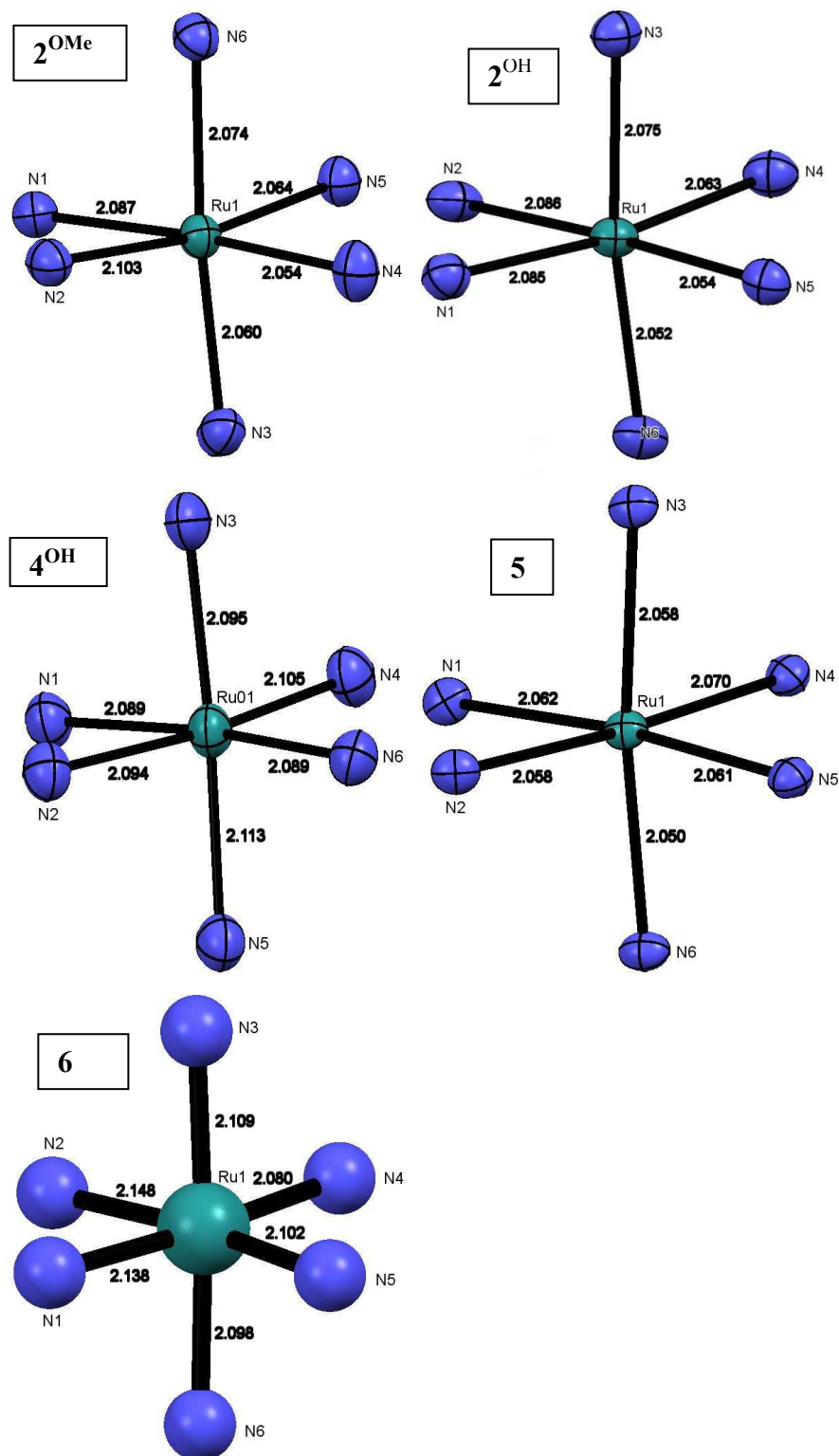


**Figure 3.** A comparison of crystal structures of complexes showing only the coordination spheres, with bond distances listed in Å. Structure **6** was reproduced from literature.<sup>24</sup> Note: Thermal ellipsoid data are not available for **6**.

**Thermodynamic Acidity.** Complex  $\mathbf{4}^{\text{OH}}$  has two acidic protons on the hydroxyl groups, so it can equilibrate between the protonated (dicationic) and deprotonated (neutral) forms depending on the solution pH. Therefore, we were interested in measuring the  $\text{p}K_{\text{a}}$  values for  $\mathbf{4}^{\text{OH}}$  by potentiometric titration. Briefly, a sample of  $\mathbf{4}^{\text{OH}}$  was dissolved in deionized water to prepare the analyte solution, which was then pre-treated with four equivalents of  $\text{HCl}_{(\text{aq})}$  to ensure that the analyte is fully protonated. The solution was then titrated with standardized base (aq. NaOH solution). Despite the fact that the compound is diprotic, only one equivalence point was observed and hence the average of two  $\text{p}K_{\text{a}}$  values was determined to be 6.08(2). This result is common in the literature for closely spaced  $\text{p}K_{\text{a}}$  values, as similar results have been reported by us and others.<sup>25-27</sup> This value is similar to literature analogs including  $\text{p}K_{\text{a}(\text{avg})} = 6.0(1)$  for  $\mathbf{2}^{\text{OH}}$  and 6.01(8) for  $\mathbf{5}$ .<sup>19</sup> Thus, moving the hydroxy groups to a different position (6,6' vs. 4,4') or adding methyl groups to the phen ligand does not appreciably change the  $\text{p}K_{\text{a}}$  values.

**Cyclic Voltammetry.** The electrochemical properties of the Ru polypyridyl complexes were investigated by cyclic voltammetry. The measurements were performed in aqueous solutions with a Britton-Robinson buffer system as electrolyte. All complexes studied exhibited reversible waves assigned to  $\text{Ru}^{\text{III/II}}$  couple (see the supporting information for CV spectra and further details). The  $E_{1/2}$  values vs. Ag/AgCl of all three new complexes are shown in Table 1. The metal based redox potentials are a great probe for the electron density on the central metal. Compared to  $\mathbf{2}^{\text{OMe}}$  and  $\mathbf{3}^{\text{OMe}}$  ( $E_{1/2} = 0.99$  and 0.98 V, respectively), the significantly lower  $E_{1/2}$  ( $\text{Ru}^{\text{III/II}}$ ) for  $\mathbf{4}^{\text{OH}}$  (0.66 V) reflects the higher electron density on Ru due to the electron-donating OH groups which are predominantly deprotonated under the experimental CV conditions (pH = 7.0, which was chosen to model physiological conditions). Similarly, the metal complexes  $[(\text{bipy})_2\text{Ru}(6,6'\text{-dhbp})]^{2+}$  ( $\mathbf{1}^{\text{OH}}$ ) and  $[(\text{bipy})_2\text{Ru}(4,4'\text{-dhbp})]^{2+}$  show  $\text{Ru}^{\text{II/III}}$  redox potentials of 1.12 V and 1.16 V vs. SCE respectively, in acetonitrile.<sup>20</sup> Deprotonation is expected to shift these potentials lower, and for  $[(\text{bipy})_2\text{Ru}(6,6'\text{-(O)}_2\text{-bipy)}]$  ( $\mathbf{1}^{\text{O}}$  in Scheme 1) an irreversible wave at 0.45 V vs. SCE in acetonitrile was observed.<sup>20</sup> Despite differences in solvent, the general trend suggests that the differences in redox potentials between  $\mathbf{2}^{\text{OMe}}$  and  $\mathbf{3}^{\text{OMe}}$  vs.  $\mathbf{4}^{\text{OH}}$  are largely due to ligand deprotonation which is only possible for  $\mathbf{4}^{\text{OH}}$ .

**Photodissociation.** All three new ruthenium complexes undergo blue light ( $\lambda = 450$  nm) induced ligand dissociation in aqueous solution. The photodissociation rate is known to be directly related to the steric bulk close to the metal center, as increasing steric strain is known to lower the energy of the  $^3\text{MC}$  state, thus making the pathway to photodissociation products more accessible.<sup>28</sup> The process was followed by UV-vis spectroscopy using actinometry to measure photons absorbed which allowed us to determine quantum yields as shown in Table 1 (see the Supporting Information for further details). To facilitate

comparison, the quantum yields of the parent analogues  $2^{\text{OH}}$  and  $3^{\text{OH}}$  are also shown in Table 1. All compounds were studied under acidic conditions (pH 5.0-5.1) to ensure that the protic complexes are present as the more photolabile dicationic species bearing OH groups. This work shows that the quantum yields increase in the order:  $3^{\text{OH}} < 4^{\text{OH}} < 2^{\text{OH}} < 3^{\text{OMe}} \ll 2^{\text{OMe}}$ . Comparing these values, the quantum yields for  $3^{\text{OH}}$ ,  $4^{\text{OH}}$ , and  $2^{\text{OH}}$  are all similar and quite low ( $\sim 10^{-3}$ ). Most surprising in this series is that  $2^{\text{OH}}$  and  $4^{\text{OH}}$  have similar quantum yields, despite the crystal structure of  $4^{\text{OH}}$  showing more distortion in the spectator ligands. Comparing  $3^{\text{OH}}$  to  $3^{\text{OMe}}$ , we observe a three-fold increase in  $\phi_{\text{PD}}$  by using the more-bulky methoxy group. Furthermore, electronics may play a role in that  $3^{\text{OH}}$  is expected to have some (49.6%) mono-deprotonated species present in solution at pH 5.0, which is expected to be less photolabile with a monoanionic ligand.<sup>19</sup> The quantum yield is highest for complex  $2^{\text{OMe}}$  at 0.024(6). Thus, a twelve-fold increase in quantum yield occurs in moving from  $2^{\text{OH}}$  to  $2^{\text{OMe}}$ . In our prior work, we showed a 56-fold increase in the quantum yield (Table 1) by going from predominantly  $2^{\text{O}^-}$  to  $2^{\text{OH}}$  by lowering the pH from 7.5 to 5.0. Thus, the change from  $2^{\text{OH}}$  to  $2^{\text{OMe}}$  can be attributed to both sterics and to eliminating the protic ligand, which at pH 5.0 for  $2^{\text{OH}}$  leads to 38.5% of the mono-deprotonated species based on the  $\text{p}K_{\text{a}}$  values.<sup>19</sup> In summary, it appears from comparing  $2^{\text{OMe}}$  and  $4^{\text{OH}}$  that steric bulk on the 6,6'-dmbp ligand (with two methoxy groups near the metal) is a more effective strategy for favoring photodissociation vs. the use of dmphen (with four methyl groups near the metal). We speculate that this may be due to the presence of steric bulk in a ligand that already has weaker Ru-N bonds due to the electronic effects of the methoxy group. It is known that the addition of OH or OMe groups *ortho* to nitrogen results in a less basic bipyridine ligand which implies a weaker Ru-N bond strengths.<sup>25, 29, 30</sup> The ease of ligand distortion is evident in terms of the tilting of the 6,6'-dmbp ligand below the equatorial plane in  $2^{\text{OMe}}$  (Figure 2).

**Cytotoxicity towards breast cancer cells.** Using the same protocol as reported previously,<sup>19</sup> breast cancer cells were incubated with the ruthenium complexes for one hour and then they were exposed to blue light or kept in dark as a comparison. The resulting  $\text{IC}_{50}$  values are shown in Table 3. All of the new compounds reported ( $2^{\text{OMe}}$ ,  $3^{\text{OMe}}$ ,  $4^{\text{OH}}$ ) are essentially non-toxic vs. MDA-MB-231 breast cancer cells. This stands in marked contrast to complex  $2^{\text{OH}}$  which had some light triggered toxicity toward certain cell lines and  $3^{\text{OH}}$  which was displayed good cytotoxicity ( $\text{IC}_{50}$  light = 3.7  $\mu\text{M}$ ) and photo-toxicity indices against several cell lines.<sup>19</sup> In our prior work, cellular uptake played a key role in determining toxicity, and thus we suspected that poor cellular uptake may be responsible for the low toxicity of  $2^{\text{OMe}}$ ,  $3^{\text{OMe}}$ , and  $4^{\text{OH}}$ .

**Table 3.** Breast cancer (MDA-MB-231) cell cytotoxicity data when treated with ruthenium complexes at pH 7.4 in the dark or upon irradiation for one hour with blue light ( $\lambda = 450$  nm). All  $IC_{50}$  values are in  $\mu M$ .

Compound	$IC_{50}$ dark	$IC_{50}$ light
<b>2</b> <sup>OMe</sup>	>100	>100
<b>3</b> <sup>OMe</sup>	>100	>100
<b>4</b> <sup>OH</sup>	>100	>100
<b>2</b> <sup>OH a</sup>	280	83
<b>3</b> <sup>OH a</sup>	190	3.7

<sup>a</sup>The  $IC_{50}$  values for both **2**<sup>OH</sup> and **3**<sup>OH</sup> have been reported previously.<sup>19</sup>

**Octanol/Water Partition Coefficients.** Octanol/water partition coefficients ( $\log(D_{o/w})$ ) provide a convenient measure by which to estimate cellular uptake by passive diffusion. Lipophilic complexes display positive  $\log(D_{o/w})$  values that are ideally between 2-6 for good cellular uptake and with sufficient water solubility for drug administration.<sup>16, 31, 32</sup> Conversely, without appreciable cellular uptake it is unlikely that a drug will generate appreciable cytotoxicity, unless the cellular membrane is compromised upon light irradiation. We measured the  $\log(D_{o/w})$  values of these compounds at pH 7.4 to simulate physiological conditions, as shown in Table 1. Complexes **2**<sup>OMe</sup> and **3**<sup>OMe</sup> are dicationic at all pH values due to the aprotic ligands. Thus, these complexes are quite hydrophilic which leads to negative  $\log(D_{o/w})$  values. In contrast, **4**<sup>OH</sup> is majority deprotonated at pH 7.4 which leads to a positive (but low)  $\log(D_{o/w})$  value of 0.58(2). Nonetheless, all three compounds appear to have  $\log(D_{o/w})$  values too low (cf. **2**<sup>OH</sup> and **3**<sup>OH</sup> in Table 1) to lead to appreciable cytotoxicity. Again, **2**<sup>OH</sup> and **3**<sup>OH</sup>, while structurally similar to **2**<sup>OMe</sup> and **3**<sup>OMe</sup>, can be deprotonated at pH 7.4 to give more lipophilic neutral species. This deprotonation appears to increase  $\log(D_{o/w})$  by over two orders of magnitude. We postulate that the low toxicity observed for these new compounds is both due to poor uptake and low toxicity for the products of photodissociation (see further discussion below).

## Conclusions

By installing methoxy groups on the *ortho* to nitrogen positions, we have made ruthenium complexes that photodissociate more readily than any of the compounds reported in our prior work. In one exemplary example, by adjusting the functional groups from **2**<sup>O-</sup> to **2**<sup>OH</sup> to **2**<sup>OMe</sup>, we are able to increase the quantum yields by 56-fold (with pH changes<sup>19</sup>) and then another 12-fold (with synthesis), for a combined quantum yield enhancement of 667-fold (to  $\phi_{PD} = 0.024(6)$  for **2**<sup>OMe</sup>). It appears that the quantum yield enhancement is due to both steric and electronic factors: namely that it is important to have the sterically bulky ligand be a weak sigma donor with inherently weak Ru-N bond strengths. Illustrating this trend,

$4^{\text{OH}}$  (with the 4,4'-dhbp ligand) displayed a relatively low quantum yield despite having four methyl groups near the metal center from the two dmphen ligands. Despite the relatively large quantum yield for  $2^{\text{OMe}}$ , it was non-toxic. This can be (partially) attributed to an unfavorable  $\log(D_{o/w})$  value which would lead to poor drug uptake by passive diffusion. Furthermore, note that  $2^{\text{OMe}}$  photodissociation leads to the same photoproduct as  $2^{\text{OH}}$ , namely  $[(\text{phen})_2\text{Ru}(\text{OH}_2)_2]^{2+}$ . Similarly,  $3^{\text{OMe}}$  photodissociation leads to  $[(\text{dop})_2\text{Ru}(\text{OH}_2)_2]^{2+}$  (same photoproduct as for  $3^{\text{OH}}$ ). Therefore, this work also leads us to question whether, in our prior work with  $2^{\text{OH}}$  and  $3^{\text{OH}}$ , these photoproducts were the true toxic species. Alternative hypotheses can include that the photo-released free ligand (e.g. 6,6'-dhbp)<sup>14</sup> was in fact toxic (we note that 6,6'-dhbp was non-toxic when administered directly to cells,<sup>19</sup> but we cannot rule out that ruthenium acts as a drug delivery vehicle) or that we were generating singlet oxygen<sup>13</sup> as a toxic species in our past work.<sup>19</sup> We note that  $3^{\text{OH}}$  had a very low quantum yield ( $2.2 \times 10^{-4}$ ) for photodissociation at physiological pH (Table 1). More effective photo dissociating ruthenium complexes will typically have quantum yields of  $10^{-1}$  to  $10^{-2}$ .<sup>6, 33</sup> We will clarify this matter with a separate publication addressing the cause of toxicity in  $3^{\text{OH}}$ . We summarize our studies of  $2^{\text{OMe}}$ ,  $3^{\text{OMe}}$ , and  $4^{\text{OH}}$  by stating that  $\log(D_{o/w})$  values are not ideal for uptake by passive diffusion and, despite excellent quantum yields, the species generated by photodissociation are not sufficiently toxic to trigger cell death from outside the cell membrane. Importantly, we have elucidated a key factor in controlling quantum yields by installing sterically bulky groups on weak donor ligands. Furthermore, these changes help to separate the contributions from sterics ( $2^{\text{OMe}}$  vs.  $2^{\text{OH}}$ ) vs. electronics ( $2^{\text{OH}}$  vs.  $2^{\text{O}^-}$ ) in determining the quantum yields and this study suggests that electronic play a dominant role in this case.

## Experimental Section

**General specifications: Materials.** All syntheses were carried out under a nitrogen atmosphere using glovebox or standard Schlenk techniques if not otherwise indicated. All commercially available reagents were purchased from Sigma-Aldrich, Acros, Strem or Pressure Chemical and were used as received without further purification. (COD)RuCl<sub>2</sub>, (phen)<sub>2</sub>RuCl<sub>2</sub>, (dop)<sub>2</sub>RuCl<sub>2</sub>, 6,6'-dmbp and 4,4'-dhbp were synthesized according to previously published procedures.<sup>19, 26, 30</sup> Dry solvents were obtained by passing through a column of activated alumina using a Glass Contour Solvent Purification System built by Pure Process Technology, LLC. pH measurements were carried out using a VWR SympHony pH meter, utilizing a three-point calibration at pH = 4, 7, and 10. Britton-Robinson buffer solutions were made from a stock solution of 0.04 M acetic acid, 0.04 M boric acid, and 0.04 M phosphoric acid with the addition of 0.2 M sodium hydroxide to achieve an approximate pH of 7 for the solution after the addition of the metal complex.

**General specifications: Instruments and Analysis.** <sup>1</sup>H and <sup>13</sup>C spectra were acquired at room temperature on a Bruker AV360 360 MHz or AV500 500 MHz spectrometer, as designated. Chemical shifts are reported in ppm and referenced to residual solvent resonance peaks. Abbreviations for the multiplicity of NMR signals are s (singlet), d (doublet), t (triplet), q (quartet), m (multiplet), br (broad). UV-visible spectra were recorded on a Perkin Elmer Lambda 35 UV-visible spectrometer. Mass spectrometric data were collected on a Waters AutoSpec-Ultima NT spectrometer with electron ionization method. ESI mass-spectrometry was provided by the University of Alabama Mass Spectrometry Resource. Elemental analyses were performed by Atlantic Microlab, Inc., Norcross, GA. Cyclic voltammetry measurements were performed on a Bioanalytical Systems CW-50 potentiostat. Typical concentrations for metal complexes ranged from 0.64 to 0.84 mM. Studies were carried out in aqueous Britton-Robinson buffer solutions as the supporting electrolyte. The pH of each solution was checked after the dissolution of metal complex for study. A three-electrode setup with an Ag/AgCl reference electrode in 3M aqueous sodium chloride (electrode model MF-2052 from Bioanalytical Systems), platinum wire auxiliary electrode, and glassy carbon working electrode was used. In all studies, the solutions were degassed for approximately 30 minutes with argon prior to data collection and the glassy carbon electrode was polished before each scan.

**[(phen)<sub>2</sub>Ru(6,6'-dmbp)]Cl<sub>2</sub> (2<sup>OMe</sup>).** A similar procedure reported for the synthesis of (phen)<sub>2</sub>Ru(6,6'-dhbp)Cl<sub>2</sub> was used.<sup>19</sup> The whole process was protected from light as the final product is sensitive to light. An oven dried Schlenk flask equipped with a stir bar was charged with 1:1 volume ratio of DI water and ethanol (40 mL overall) and was purged with nitrogen for 20 minutes. (phen)<sub>2</sub>RuCl<sub>2</sub> (0.1010 g, 0.1878 mmol) and 6,6'-dimethoxy-2,2'-bipyridine (0.0454 g, 0.2066 mmol, 1.1 eq) were measured into the flask. The final dark brown suspension was heated to reflux in an oil bath at 110 °C under N<sub>2</sub> for 24 h. After cooling down, the solution was filtered to remove any excess 6,6'-dmbp ligand. Solvent was removed by rotary evaporation. The product was collected by vacuum filtration with a diethyl ether wash. Yield: 0.0784 g, 0.1047 mmol, 56%. The crude product was purified by recrystallization from acetonitrile solution by slow diffusion of ether. <sup>1</sup>H NMR (500 MHz, CD<sub>3</sub>CN) δ 8.70 (dd, *J* = 8.3, 1.3 Hz, 2H), 8.44 (dd, *J* = 8.2, 1.3 Hz, 2H), 8.38 (dd, *J* = 5.3, 1.3 Hz, 2H), 8.27 (m, 4H), 8.19 (d, *J* = 8.9 Hz, 2H), 8.03 (dd, *J* = 8.5, 7.8 Hz, 2H), 7.84 (dd, *J* = 8.3, 5.2 Hz, 2H), 7.64 (dd, *J* = 5.3, 1.3 Hz, 2H), 7.40 (dd, *J* = 8.2, 5.3 Hz, 2H), 6.82 (dd, *J* = 8.5, 1.3 Hz, 2H), 2.86 (s, 6H). <sup>13</sup>C NMR (126 MHz, CD<sub>3</sub>CN) δ 170.48 (s), 158.00 (s), 154.61 (s), 153.18 (s), 149.83 (s), 149.35 (s), 142.04 (s), 137.38 (s), 136.49 (s), 131.75 (s), 131.28 (s), 128.87 (s), 128.62 (s), 126.79 (s), 125.88 (s), 118.55 (s), 56.99 (s). Elem. Anal.: Found: C, 53.16; N, 10.40; and H, 4.44%. Calc. for [(phen)<sub>2</sub>Ru(6,6'-dmbp)]Cl<sub>2</sub>·4H<sub>2</sub>O, C<sub>36</sub>H<sub>36</sub>Cl<sub>2</sub>N<sub>6</sub>O<sub>6</sub>Ru: C, 52.69; N, 10.24; and H, 4.42%. ESI-MS (*m/z*): 339.1, Calcd for [(phen)<sub>2</sub>Ru(6,6'-dmbp)]<sup>2+</sup>, [C<sub>36</sub>H<sub>28</sub>N<sub>6</sub>O<sub>2</sub>Ru]<sup>2+</sup>: 339.1.

**[(dop)<sub>2</sub>Ru(6,6'-dmbp)]Cl<sub>2</sub> (3<sup>OMe</sup>)**. A similar procedure reported for the synthesis of (phen)<sub>2</sub>Ru(6,6'-dhbp)Cl<sub>2</sub> was used.<sup>19</sup> The whole process was protected from light as the final product is sensitive to light. An oven dried Schlenk flask equipped with a stir bar charged with 1:1 volume ratio of DI water and ethanol (20 mL overall) and was purged with nitrogen for 20 minutes. (dop)<sub>2</sub>RuCl<sub>2</sub> (0.0455 g, 0.0694 mmol) and 6,6'-dimethoxy-2,2'-bipyridine (0.0178 g, 0.0763 mmol, 1.1 eq) were measured into the flask. The final dark brown suspension was heated to reflux in an oil bath at 110 °C under N<sub>2</sub> for 24 h. After cooling down, the solution was filtered to remove any excess 6,6'-dmbp ligand. Solvent was removed by rotary evaporation. The product was collected by vacuum filtration with a diethyl ether wash. The crude product was purified by recrystallization from acetonitrile solution by slow diffusion of ether. Yield: 0.0490 g, 0.0567 mmol, 81.6%. <sup>1</sup>H NMR (500 MHz, CD<sub>3</sub>CN) δ 8.63 (dd, *J* = 8.4, 1.3 Hz, 2H), 8.40 (dd, *J* = 8.4, 1.3 Hz, 2H), 8.22 (m, 4H), 8.03 (t, *J* = 8.3, 2H), 7.75 (dd, *J* = 8.4, 5.2 Hz, 2H), 7.50 (dd, *J* = 5.3, 1.3 Hz, 2H), 7.35 (dd, *J* = 8.3, 5.3 Hz, 1H), 6.83 (d, 2H), 4.62 (m, 4H), 2.91 (s, 6H). <sup>13</sup>C NMR (126 MHz, CD<sub>3</sub>CN) δ 170.41 (s), 157.93 (s), 152.44 (s), 151.05 (s), 145.39 (s), 144.92 (s), 141.98 (s), 135.60 (s), 135.41 (s), 130.05 (s), 129.18 (s), 126.28 (s), 125.95 (s), 125.43 (s), 125.41 (s), 109.33 (s), 66.20 (s), 57.04 (s). Elem. Anal.: Found: C, 50.75; N, 8.98; and H, 4.37%. Calc. for [(dop)<sub>2</sub>Ru(6,6'-dmbp)]Cl<sub>2</sub>·5H<sub>2</sub>O, C<sub>40</sub>H<sub>42</sub>Cl<sub>2</sub>N<sub>6</sub>O<sub>11</sub>Ru: C, 50.32; N, 8.80; and H, 4.43%. ESI-MS (*m/z*): 829.1, Calcd for [(dop)<sub>2</sub>Ru(6,6'-dmbp) Cl]<sup>+</sup>, [C<sub>40</sub>H<sub>32</sub>ClN<sub>6</sub>O<sub>6</sub>Ru]<sup>+</sup>: 829.1; 779.2, Calcd for [(dop)<sub>2</sub>Ru(6,6'-dmbp) – CH<sub>3</sub>]<sup>+</sup>, [C<sub>39</sub>H<sub>29</sub>N<sub>6</sub>O<sub>6</sub>Ru]<sup>+</sup>: 779.1; 397.2, Calcd for [(dop)<sub>2</sub>Ru(6,6'-dmbp)]<sup>2+</sup>, [C<sub>40</sub>H<sub>32</sub>N<sub>6</sub>O<sub>6</sub>Ru]<sup>2+</sup>: 397.1.

**[(dmphen)<sub>2</sub>Ru(4,4'-dhbp)]Cl<sub>2</sub> (4<sup>OH</sup>)** The compound [(dmphen)<sub>2</sub>Ru(4,4'-dhbp)](PF<sub>6</sub>)<sub>2</sub> was made by following a similar procedure as reported previously.<sup>20</sup> 40 mL of ethylene glycol was degassed with argon for 30 min in a round-bottom flask. To the flask, 4,4'-dhbp (0.1762 g, 0.936 mmol) and previously synthesized Ru(dmphen)<sub>2</sub>Cl<sub>2</sub> (0.4076 g, 0.693 mmol) were added. The solution was heated to 190°C under argon for 4 h. The solution turned a deep red as the reaction proceeded. The solution was removed from heat and cooled to room temperature, followed by filtration through a Büchner funnel to remove insoluble impurities. Five-fold excess (0.8128 g) of ammonium hexafluorophosphate was dissolved in 20 mL of water and added to the filtrate to precipitate the PF<sub>6</sub><sup>-</sup> salt. The solution was filtered and left to sit on vacuum overnight. The next day the remaining powder was rinsed with ether. [Ru(dmphen)<sub>2</sub>(4,4'-dhbp)](PF<sub>6</sub>)<sub>2</sub>·4H<sub>2</sub>O (0.6206 g, 0.581 mmol) was collected (83.8% yield). It was then converted to the chloride salt in the following way: the PF<sub>6</sub><sup>-</sup> salt (210 mg) was measured into a 100 mL flask with 50 mL of acetone. The solution was stirred in dark for 20 minutes. The solution was filtered to remove the undissolved powder. To the clear red filtrate, saturated Et<sub>4</sub>NCl in acetone was added, until no further precipitate was formed. The red precipitate was collected by filtration, washed with acetone, ether, and then dried under vacuum. Crystals suitable for X-ray analysis were grown by slow diffusion of ether into the ethanol solution of the compound. <sup>1</sup>H NMR (500 MHz, DMSO) δ 12.03 (br, 2H), 8.79 (d, *J* = 8.3 Hz, 2H), 8.52 (d, *J* = 8.3 Hz, 2H), 8.34 (d, *J* = 8.7 Hz, 2H), 8.23 (d, *J* = 8.8 Hz, 2H), 7.87 (d, *J* = 8.3 Hz, 2H), 7.68 (s, 2H), 7.61 (d, *J* = 8.3 Hz, 2H), 6.51 (m, 4H), 1.99 (s, 6H), 1.83 (s, 6H). <sup>13</sup>C NMR (126 MHz, DMSO) δ 167.60 (s), 165.90 (s), 165.84 (s), 157.85 (s), 151.54 (s), 149.00 (s), 148.11 (s), 137.38 (s), 136.42 (s), 129.28 (s), 127.32 (s), 126.97 (s), 126.90 (s), 126.56 (s), 114.63 (s), 111.34 (s), 25.74 (s), 24.32 (s). Elem. Anal.: Found: C, 54.75; N, 9.72; and H, 4.84%. Calc. for [(dmphen)<sub>2</sub>Ru(4,4'-dhbp)]Cl<sub>2</sub>·EtOH·3H<sub>2</sub>O, C<sub>44</sub>H<sub>44</sub>Cl<sub>2</sub>N<sub>6</sub>O<sub>6</sub>Ru: C, 54.79; N, 9.59; and H, 5.06%. ESI-MS (*m/z*): 353.2, Calcd for [(dmphen)<sub>2</sub>Ru(4,4'-dhbp)]<sup>2+</sup>, [C<sub>38</sub>H<sub>32</sub>N<sub>6</sub>O<sub>2</sub>Ru]<sup>2+</sup>: 353.1.

**Single Crystal X-Ray Diffraction (SC-XRD) Structure Determinations.** Crystals of appropriate dimension were mounted on a Mitgen cryoloop or glass filament in a random orientation. Preliminary examination and data collection were performed on a Bruker ApexII CCD-based X-ray diffractometer equipped with an Oxford N-Helix Cryosystem low temperature device and a fine focus Mo-target X-ray tube ( $\lambda = 0.71073 \text{ \AA}$ ) operated at 1500 W power (50 kV, 30 mA). The X-ray intensities were measured at low temperature (223 (2) K). The collected frames were integrated with the Saint<sup>34</sup> software using a narrow-frame algorithm. Data were corrected for absorption effects using the multi-scan method in

SADABS.<sup>35</sup> The space groups were assigned using XPREP of the Bruker ShelXTL package,<sup>36</sup> solved with ShelXT<sup>36</sup> and refined with ShelXL<sup>36</sup> and the graphical interface ShelXle.<sup>37</sup> All non-hydrogen atoms were refined anisotropically. H atoms attached to carbon were positioned geometrically and constrained to ride on their parent atoms.

The structure of **4<sup>OH</sup>** was found to contain several regions of residual density. Attempts to model the remaining residual density as ethanol molecules were not successful, so the residual density was “SQUEEZED” (i.e., applied a “solvent mask”) out using the PLATON program.<sup>38</sup> The solvent accessible volume was found to be 520 Å<sup>3</sup>. The electrons found in solvent accessible void is 135 e<sup>-</sup>, which corresponds to approximately 5 ethanol molecules per asymmetric unit. Hydroxyl H atom positions were restrained based on hydrogen bonding considerations (DFIX and DANG).

**Cell culture:** MDA-MB-231 cell line was purchased from American Type Culture Collection (ATCC). MDA-MB-231 cells of less than 10 passages were grown using DMEM (Gibco, 21063-029) supplemented with 10% FBS (Gibco, 26140079).

**Determination of the IC<sub>50</sub> values for 2<sup>OMe</sup>, 3<sup>OMe</sup>, and 4<sup>OH</sup>.** MDA-MB-231 (ATCC, HTB-26) cells were grown with DMEM (Gibco, 21063-029) supplemented with 10% fetal bovine serum (Gibco, 26140079) at 37°C with 5% CO<sub>2</sub>. IC<sub>50</sub> values were determined as reported previously.<sup>19</sup> Briefly, MDA-MB-231 cells were seeded in 96-well plates with 5,000 cells per well and incubated for 24 h. The ruthenium compounds were dissolved in dimethyl sulfoxide (DMSO) and serially diluted in media. Final DMSO concentration was lower than 0.1% to prevent any cytotoxicity from DMSO. After 24 h of incubation, the diluted compounds were added to each well and incubated for 48 h. Cells were washed with phosphate buffer saline (PBS) twice and fed with fresh media. The plate was irradiated by blue light (Phillips, goLITE BLU) for an hour and incubated overnight. Cell Counting Kit-8 (Enzo Life Sciences) was used to determine cell viability. IC<sub>50</sub> values were determined using nonlinear regression in Minitab 17.

### Conflicts of Interest

There are no conflicts to declare.

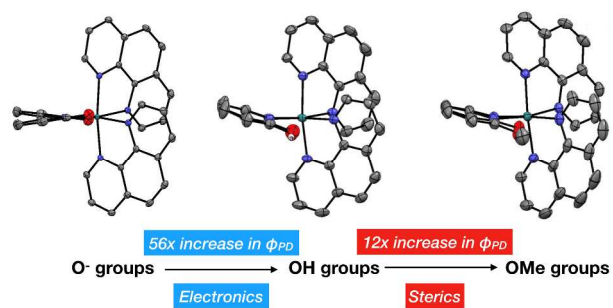
### Acknowledgements

We thank the Undergraduate Creativity and Research Academy (UCRA) at UA, the Research Grants Committee (RGC) at UA to ETP and YK, and NSF EPSCoR Track 2 Grant to ETP and RHS for support (PI: N. Hammer, Grant OIA-1539035), the University of Alabama (ETP and YK), and Villanova University (JJP) for generous financial support. We also thank Qiaoli Liang (the University of Alabama) for MS analysis. Finally, we thank M. K. Thompson and S. A. McFarland for helpful discussion and the members of the Papish group for assistance and suggestions. We thank Jessica L. Gray for assistance with measuring log(D<sub>o/w</sub>) values.

## Notes and References

1. Abbreviations: PACT = photo-activated chemotherapy, 6,6'-dhbp = 6,6'-dihydroxybipyridine, 6,6'-dmbp = 6,6'-dimethoxybipyridine, phen = 1,10-phenanthroline, dop = 2,3-dihydro-[1,4]dioxino[2,3-f][1,10]phenanthroline, dmphen = 2,9-dimethyl-1,10-phenanthroline, 4,4'-dhbp = 4,4'-dihydroxybipyridine, bipy = 2,2'-bipyridine.
2. E. Wachter, A. Zamora, D. K. Heidary, J. Ruiz and E. C. Glazer, *Chem. Commun.*, 2016, **52**, 10121-10124.
3. A. N. Hidayatullah, E. Wachter, D. K. Heidary, S. Parkin and E. C. Glazer, *Inorg. Chem.*, 2014, **53**, 10030-10032.
4. B. S. Howerton, D. K. Heidary and E. C. Glazer, *J. Am. Chem. Soc.*, 2012, **134**, 8324-8327.
5. L. M. Loftus, J. K. White, B. A. Albani, L. Kohler, J. J. Kodanko, R. P. Thummel, K. R. Dunbar and C. Turro, *Chem. Eur. J.*, 2016, **22**, 3704-3708.
6. R. N. Garner, J. C. Gallucci, K. R. Dunbar and C. Turro, *Inorg. Chem.*, 2011, **50**, 9213-9215.
7. A. Li, J. K. White, K. Arora, M. K. Herroon, P. D. Martin, H. B. Schlegel, I. Podgorski, C. Turro and J. J. Kodanko, *Inorg. Chem.*, 2016, **55**, 10-12.
8. K. Arora, J. K. White, R. Sharma, S. Mazumder, P. D. Martin, H. B. Schlegel, C. Turro and J. J. Kodanko, *Inorg. Chem.*, 2016, **55**, 6968-6979.
9. C. Gaiddon and M. Pfeffer, *Eur. J. Inorg. Chem.*, 2017, **2017**, 1-17.
10. Z. Liu and P. J. Sadler, *Acc. Chem. Res.*, 2014, **47**, 1174-1185.
11. L. Zeng, Y. Chen, H. Huang, J. Wang, D. Zhao, L. Ji and H. Chao, *Chem. Eur. J.*, 2015, **21**, 15308-15319.
12. H. R. Bautista, R. O. S. Díaz, L. Q. Shen, C. Orvain, C. Gaiddon, R. Le Lagadec and A. D. Ryabov, *J. Inorg. Biochem.*, 2016, **163**, 28-38.
13. T. Sainuddin, J. McCain, M. Pinto, H. Yin, J. Gibson, M. Hetu and S. A. McFarland, *Inorg. Chem.*, 2016, **55**, 83-95.
14. J.-A. Cuello-Garibo, M. S. Meijer and S. Bonnet, *Chem. Commun.*, 2017, **53**, 6768-6771.
15. M. Huisman, J. K. White, V. G. Lewalski, I. Podgorski, C. Turro and J. J. Kodanko, *Chem. Commun.*, 2016, **52**, 12590-12593.
16. S. Tardito, I. Bassanetti, C. Bignardi, L. Elviri, M. Tegoni, C. Mucchino, O. Bussolati, R. Franchi-Gazzola and L. Marchiò, *J. Am. Chem. Soc.*, 2011, **133**, 6235-6242.
17. A. V. Rudnev, L. S. Foteeva, C. Kowol, R. Berger, M. A. Jakupec, V. B. Arion, A. R. Timerbaev and B. K. Keppler, *J. Inorg. Biochem.*, 2006, **100**, 1819-1826.
18. F. Bacher, O. Dömötör, M. Kaltenbrunner, M. Mojović, A. Popović-Bijelić, A. Gräslund, A. Ozarowski, L. Filipovic, S. Radulović, É. A. Enyedy and V. B. Arion, *Inorg. Chem.*, 2014, **53**, 12595-12609.
19. F. Qu, S. Park, K. Martinez, J. L. Gray, F. S. Thowfeik, J. A. Lundeen, A. E. Kuhn, D. J. Charboneau, D. L. Gerlach, M. M. Lockart, J. A. Law, K. L. Jernigan, N. Chambers, M. Zeller, N. A. Piro, W. S. Kassel, R. H. Schmehl, J. J. Paul, E. J. Merino, Y. Kim and E. T. Papish, *Inorg. Chem.*, 2017, **56**, 7519-7532.
20. K. T. Hufziger, F. S. Thowfeik, D. J. Charboneau, I. Nieto, W. G. Dougherty, W. S. Kassel, T. J. Dudley, E. J. Merino, E. T. Papish and J. J. Paul, *J. Inorg. Biochem.*, 2014, **130**, 103-111.
21. E. T. Papish, J. J. Paul and E. J. Merino, 2014, Patent Application filed with US Patent Office
22. R. A. Cardone, V. Casavola and S. J. Reshkin, *Nat. Rev. Cancer*, 2005, **5**, 786-795.
23. C. M. Boudreaux, N. P. Liyanage, H. Shirley, S. Siek, D. L. Gerlach, F. Qu, J. H. Delcamp and E. T. Papish, *Chem. Commun.*, 2017, **53**, 11217-11220.
24. G. Yang, L. Ji, X. Zhou and Z. Zhou, *Transition Met. Chem.*, 1998, **23**, 273-276.
25. D. L. Gerlach, S. Bhagan, A. A. Cruce, D. B. Burks, I. Nieto, H. T. Truong, S. P. Kelley, C. J. Herbst-Gervasoni, K. L. Jernigan, M. K. Bowman, S. Pan, M. Zeller and E. T. Papish, *Inorg. Chem.*, 2014, **53**, 12689-12698.
26. J. DePasquale, I. Nieto, L. E. Reuther, C. J. Herbst-Gervasoni, J. J. Paul, V. Mochalin, M. Zeller, C. M. Thomas, A. W. Addison and E. T. Papish, *Inorg. Chem.*, 2013, **52**, 9175-9183.
27. Y. Himeda, *Eur. J. Inorg. Chem.*, 2007, **2007**, 3927-3941.
28. J. K. White, R. H. Schmehl and C. Turro, *Inorg. Chim. Acta*, 2017, **454**, 7-20.
29. D. B. Burks, M. Vasiliu, D. A. Dixon and E. T. Papish, *The Journal of Physical Chemistry A*, 2018, **122**, 2221-2231.

30. D. C. Marelius, S. Bhagan, D. J. Charboneau, K. M. Schroeder, J. M. Kamdar, A. R. McGettigan, B. J. Freeman, C. E. Moore, A. L. Rheingold, A. L. Cooksy, D. K. Smith, J. J. Paul, E. T. Papish and D. B. Grotjahn, *Eur. J. Inorg. Chem.*, 2014, **2014**, 676-689.
31. M. V. Babak, S. M. Meier, K. V. M. Huber, J. Reynisson, A. A. Legin, M. A. Jakupec, A. Roller, A. Stukalov, M. Gridling, K. L. Bennett, J. Colinge, W. Berger, P. J. Dyson, G. Superti-Furga, B. K. Keppler and C. G. Hartinger, *Chemical Science*, 2015, **6**, 2449-2456.
32. L. Tabrizi and H. Chiniforoshan, *Dalton Trans.*, 2016, **45**, 18333-18345.
33. L. Kohler, L. Nease, P. Vo, J. Garofolo, D. K. Heidary, R. P. Thummel and E. C. Glazer, *Inorg. Chem.*, 2017, **56**, 12214-12223.
34. Bruker AXS Inc., Madison, Wisconsin, USA, 2007.
35. Bruker AXS Inc., Madison, Wisconsin, USA, 2001
36. G. M. Sheldrick, *Acta Cryst.*, 2008, **A64**, 112-122.
37. C. B. Hübschle, G. M. Sheldrick and B. Dittrich, *J. Appl. Cryst.*, 2011, **44**, 1281-1284.
38. A. L. Spek, *Acta crystallographica. Section D, Biological crystallography*, 2009, **65**, 148-155.

**Table of Contents Graphic:**

**Synopsis:** Ruthenium complexes exhibit enhanced photodissociation quantum yields due to bulky, weak donor ligands, illustrating the impact of electronics and sterics.